Insect Biochemistry and Molecular Biology 52 (2014) 1–12

Contents lists available at ScienceDirect

Insect Biochemistry and Molecular Biology

journal homepage: www.elsevier.com/locate/ibmb

β-chain of ATP synthase as a lipophorin binding protein and its role in lipid transfer in the midgut of *Panstrongylus megistus* (Hemiptera: Reduviidae)

Leonardo L. Fruttero [a, 1], Diogo R. Demartini [b], Edilberto R. Rubiolo [a], Célia R. Carlini [b, c, 3], Lilián E. Canavoso [a, *, 2]

[a] Departamento de Bioquímica Clínica, Centro de Investigaciones en Bioquímica Clínica e Inmunología (CIBICI-CONICET), Facultad de Ciencias Químicas-Universidad Nacional de Córdoba, Córdoba, CP 5000, Argentina
[b] Graduate Program in Cellular and Molecular Biology, Center of Biotechnology, Universidade Federal do Rio Grande do Sul, Porto Alegre, Brazil
[c] Department of Biophysics, Universidade Federal do Rio Grande do Sul, Porto Alegre, Brazil

ARTICLE INFO

Article history:
Received 13 January 2014
Received in revised form
30 May 2014
Accepted 10 June 2014
Available online 19 June 2014

Keywords:
Triatominae
Midgut
Lipid metabolism
Lipophorin receptors
β-chain of ATP synthase

ABSTRACT

Lipophorin, the main lipoprotein in the circulation of the insects, cycles among peripheral tissues to exchange its lipid cargo at the plasma membrane of target cells, without synthesis or degradation of its apolipoprotein matrix. Currently, there are few characterized candidates supporting the functioning of the docking mechanism of lipophorin-mediated lipid transfer. In this work we combined ligand blotting assays and tandem mass spectrometry to characterize proteins with the property to bind lipophorin at the midgut membrane of *Panstrongylus megistus*, a vector of Chagas' disease. We further evaluated the role of lipophorin binding proteins in the transfer of lipids between the midgut and lipophorin. The β subunit of the ATP synthase complex (β-ATPase) was identified as a lipophorin binding protein. β-ATPase was detected in enriched midgut membrane preparations free of mitochondria. It was shown that β-ATPase partially co-localizes with lipophorin at the plasma membrane of isolated enterocytes and in the sub-epithelial region of the midgut tissue. The interaction of endogenous lipophorin and β-ATPase was also demonstrated by co-immunoprecipitation assays. Blocking of β-ATPase significantly diminished the binding of lipophorin to the isolated enterocytes and to the midgut tissue. *In vivo* assays injecting the β-ATPase antibody significantly reduced the transfer of [^{3}H]-diacylglycerol from the midgut to the hemolymph in insects fed with [9,10-^{3}H]-oleic acid, supporting the involvement of lipophorin-β-ATPase association in the transfer of lipids. In addition, the β-ATPase antibody partially impaired the transfer of fatty acids from lipophorin to the midgut, a less important route of lipid delivery to this tissue. Taken together, the findings strongly suggest that β-ATPase plays a role as a docking lipophorin receptor at the midgut of *P. megistus*.

1. Introduction

Lipophorin, a high-density lipoprotein, is the main lipid carrier in insect hemolymph. It is composed of two structural apolipoproteins, apolipophorin I and II and has a core of neutral lipids, being diacylglycerol the major lipid class. Lipophorin also transports sterols, cuticular hydrocarbons, carotenoids and other lipids (Canavoso et al., 2001).

Lipophorin executes both, endogenous and exogenous lipid transport by carrying dietary lipids from the midgut to the fat body and also distributing stored or biosynthesized lipids to peripheral tissues thus working as a reusable shuttle (Van der Horst et al., 2009). The functioning of this selective lipid transfer resides in a

Abbreviations: Bodipy-FA, 4,4-difluoro-5,7-dimethyl-4-bora-3a,4a-diaza-s-indacene-3-hexadecanoic acid; β-ATPase, β subunit of the ATP synthase complex; BSA, Bovine Serum Albumin; DiI, 1,10-dioctadecyl-3,3,30,30-tetramethylindocarbocyanine; HDL, High Density Lipoprotein; JHBP, juvenile hormone binding protein; Lp, Lipophorin; LpR, lipophorin receptor; LC-ESI-QTOF, Liquid Chromatography-Electrospray Ionization-Quadrupole Time of flight; LDLR, Low Density Lipoprotein Receptor; MS/MS, tandem mass spectrometry.

* Corresponding author. Tel.: +54 351 5353850; fax: +54 351 433 3048.
E-mail address: lcanavo@mail.fcq.unc.edu.ar (L.E. Canavoso).

[1] Research Fellow from CONICET-Argentina.
[2] Member of the CIC-CONICET-Argentina.
[3] Present address: Instituto do Cérebro - InsCer, Pontifícia Universidade Católica do Rio Grande do Sul, Av. Ipiranga 6690, Porto Alegre, Brazil.

http://dx.doi.org/10.1016/j.ibmb.2014.06.002
0965-1748/

docking mechanism by which lipophorin, bound to a receptor, transfers lipids to/from the cell at the level of the plasma membrane without endocytosis and degradation of its protein subunits (Downer and Chino, 1985). Alternatively, as it was demonstrated in the fat body of *Locusta migratoria,* lipophorin can be internalized by the cells and resecreted into the circulation thus contributing to its recycling (Van Hoof et al., 2005).

Despite the fact that the interaction of lipophorin with specific binding sites at the membrane of the cells has been characterized in several species (Van Antwerpen et al., 1988; Tsuchida and Wells, 1990; Bauerfeind and Komnick, 1992; Dantuma et al., 1996; Grillo et al., 2003; Lee et al., 2003; Fruttero et al., 2009), the identification of lipophorin docking receptors has been poorly successful. Recently, it has been reported that Cameo2 and SCRB15, two protein members of the CD36 family, may function as non-internalizing lipophorin receptors and/or transmembrane transporters facilitating the selective uptake of carotenoids in the silk gland of *Bombyx mori* (Sakudoh et al., 2010, 2013). Conversely, the endocytic lipophorin receptor (LpR) which belongs to the superfamily of Low Density Lipoprotein Receptors (LDLR) has been cloned and sequenced in many insect species although its physiological relevance is not completely understood (Dantuma et al., 1999; Tufail and Takeda, 2009; Van der Horst et al., 2009). In *L. migratoria*, inhibition of endocytosis did not affect the transfer of diacylglycerol to fat body cells (Dantuma et al., 1997, 1999). LpRs also participates in a minor pathway of lipid delivery to the oocytes during vitellogenesis (Ziegler and Van Antwerpen, 2006). In *Drosophila melanogaster,* the expression of two lipophorin receptors, Lpr1 and Lpr2, is necessary for the accumulation of neutral lipids in oocytes and imaginal disc cells. However, insects lacking the corresponding genes were viable and stored similar amounts of body lipids as the wild type insects (Parra-Peralbo and Culi, 2011), suggesting the need of another molecular factor(s) mediating lipophorin binding and neutral lipid transfer to the target cells. Also in *D. melanogaster*, the interaction of lipophorin with two membrane-associated heparan sulfate proteoglycans, Dally and Dally-like was reported. Such interaction seems to be involved in cell signaling, due to the fact that lipophorin can carry morphogens implicated in pattern formation during development rather than in lipid transfer (Eugster et al., 2007).

F_1F_O adenosine triphosphate synthase (ATPase) is a multisubunit enzyme highly conserved throughout evolution. It is comprised of a soluble F_1 portion that contains several subunits, including α and β. The F_1F_O ATPase complex catalyzes the synthesis of ATP from ADP and inorganic phosphate in most living organisms (Walker, 1998). Nevertheless, in the absence of a proton gradient, the enzyme also functions as an ATP hydrolase (Meier et al., 2011). The ATPase complex is located in the inner membrane of the mitochondria, the thylakoid membrane of plant chloroplasts and on the plasma membrane of certain bacteria (Arechaga and Jones, 2001; Andries et al., 2005). However, in the last two decades, several reports have described the presence of various subunits of ATPase located in the surface of the cells; thus the term "ectopic ATP synthase" emerged to name this complex (Chi and Pizzo, 2006). Cell surface ATPase mediates different biological activities such as hepatic High Density Lipoprotein (HDL) cholesterol uptake, endothelial cell proliferation and tumor recognition, among others (Vantourout et al., 2010). In *Galleria mellonella*, the α and β subunits of the ATPase complex present in the membrane of fat body cells can bind the juvenile hormone binding protein (JHBP) (Zalewska et al., 2009). In *D. melanogaster*, the α-ATPase was described as a lipophorin binding protein (Giot et al., 2003). The α and β-ATPase subunits were also detected in the plasma membrane of midgut and salivary gland cells of several hemipteran species that act as vectors of phytoplasmas, a kind of phytopathogenic bacteria (Galetto et al., 2011).

The hematophagous insect *Panstrongylus megistus* is an important vector of Chagas' disease in South America that belongs to the Triatominae subfamily (Schofield et al., 2006). As most triatomines, *P. megistus* takes large blood meals containing abundant lipids. After blood feeding, phosphatidate phosphohydrolase and triacylglycerol lipase play a key role in regulating intracellular diacylglycerol synthesis in the midgut as well as its export to the hemolymph via lipophorin (Canavoso et al., 2004a). The biochemical and cellular characterization of lipophorin-midgut interaction in *P. megistus* was reported and the lack of an endocytic pathway for lipophorin in this tissue was also demonstrated (Fruttero et al., 2009).

In order to better understand the process of lipid transfer at the midgut of *P. megistus* we identified and characterized lipophorin binding proteins in the plasma membrane of this tissue, which in turn could function as lipophorin docking receptor/s. The results showed that the β-chain of the ATP synthase complex (termed β-ATPase) mediates the lipophorin binding to both, isolated enterocytes and midgut tissue. Moreover, *in vivo* blocking β-ATPase significantly impaired the transfer of radiolabeled diacylglycerol from the midgut to lipohorin, thus supporting the physiological role of β-ATPase-lipophorin association. Altogether, the findings prompted us to propose that β-ATPase plays a role as a docking lipophorin receptor in the midgut tissue of *P. megistus*.

2. Materials and methods

2.1. Chemicals

4',6-diamidino-2-phenylindole (DAPI); 4,4-difluoro-5,7-dimethyl-4-bora-3a,4a-diaza-s-indacene-3-hexadecanoic acid (Bodipy FL C16) and goat anti-rabbit IgG labeled with Alexa 568 antibody (Molecular Probes, Eugene, OR, USA), rabbit anti-ATP5B/β-chain of ATP synthase of human origin (catalog code sc-33618) and rabbit anti-cytochrome *c* of equine origin (Santa Cruz Biotechnology, Inc., Santa Cruz, CA, USA); Sephadex G-25 PD-10 columns (GE Healthcare, Little Chalfont, United Kingdom); Tissue-Tek embedding medium Optimal Cutting Temperature (OCT) (Miles, Elkhart, IN, USA); cell strainers (Becton Dickinson, Franklin Lakes, NJ, USA); enhanced chemiluminescence (ECL) detection kit (PerkinElmer, Waltham, MA, USA); electrophoresis protein standards (New England Biolabs, Ipswich, MA, USA); Moloney Murine Leukemia Virus Reverse Transcriptase (M-MLV RT) and sequencing grade modified trypsin (Promega, Madison, WI, USA); Centricon devices (Millipore, Bedford, MA, USA); 3,3′-Dithiobis(sulfosuccinimidylpropionate) (DTSSP) (Pierce Biotechnology, Rockford, IL, USA); Fluorsave (Calbiochem, Darmstadt, Germany); [9,10-^{3}H]-oleic acid (PerkinElmer New England Nuclear, Waltham, MA, USA); silica gel plates and solvents (J.T. Baker Avantor, Center Valley, PA, USA) and lipid standards (Avanti Polar Lipids, Alabaster, AL, USA) were from the indicated commercial sources. All other chemicals were from Sigma–Aldrich (St. Louis, MO, USA).

2.2. Insects

Insects were taken from a colony of *P. megistus* which is maintained under standardized rearing conditions (28 °C, 70% relative humidity, 8:16 h light:dark photoperiod) and fed fortnightly on hens blood (Canavoso and Rubiolo, 1995), according to the recommendations of the National Institute of Parasitology (Health Ministry, Argentina) (Núñez and Segura, 1987).

With the exception of the assays directed to evaluate the transfer of lipids from the midgut to lipophorin, which were performed by feeding fifth instar nymphs of *P. megistus* 10 days after molting on an artificial feeder, all the experiments were carried out

using fifth instar nymphs, 10 days after the insects received a blood meal. Unless otherwise stated, insects that consumed a blood meal of approximately twofold their body weight (240 ± 15 mg) were selected for the experiments (Canavoso et al., 2004a; Fruttero et al., 2009).

2.3. Lipophorin purification and fluorescent labeling

Lipophorin was isolated from the hemolymph of fifth instar nymphs by KBr gradient ultracentrifugation followed by fractionation on Sepharose 6B as described elsewhere (Fruttero et al., 2009).

For the *in vivo* functional experiments, lipophorin was labeled in its phospholipid moiety with the non-exchangeable fluorophore DiI (Lp-DiI) (Via and Smith, 1986) as described previously (Fruttero et al., 2009). Lipophorin was also labeled on its exchangeable lipid fraction with the fluorescent palmitic acid analog Bodipy FL C16 (Lp-Bodipy-FA) (Martin-Nizard et al., 1987; Fruttero et al., 2011). DiI and Bodipy-FA labeled lipophorin were passed through PD-10 columns to remove the free fluorophore from the fluorescently labeled ligand.

2.4. Preparation of anti-lipophorin antibody and labeling with FITC

Anti-lipophorin antibody was obtained by inoculating New Zealand rabbits with purified lipophorin as described previously (Canavoso and Rubiolo, 1995). For the immunofluorescence assays, anti-lipophorin antibody was labeled with fluorescein isothiocyanate (anti-Lp-FITC, 5 mg/ml) in dimethyl sulfoxide according to Hermanson (1996).

2.5. Isolation of midgut membranes for the ligand blotting assays

Midgut membranes were obtained by dissecting the anterior midgut under cold phosphate buffered saline (PBS: 6.6 mM Na_2HPO_4/KH_2PO_4, 150 mM NaCl, pH 7.4). After removal of the luminal contents, the midguts were extensively washed with PBS and then, homogenized using a Potter-Elvehjen homogenizer in Tris–HCl buffer (20 mM Tris, 150 mM NaCl, 2 mM $MgCl_2$, pH 7.4) in the presence of protease inhibitors. Homogenates were centrifuged at 1000 × *g* to remove large debris and then, supernatants were subjected to ultracentrifugation (106,000 × *g*, 1 h at 4 °C) (Fruttero et al., 2009). The pellets containing the membrane preparations were suspended in Tris–HCl buffer and stored at −80 °C to be used during a week, previous protein determination using BSA as standard (Bradford, 1976).

Ligand blotting assays were performed as described previously (Fruttero et al., 2009). Briefly, after the membrane preparation was fractionated by Tris-Tricine-SDS gel electrophoresis (8.5%), proteins were transferred onto a nitrocellulose membrane followed by a blocking step with Tris buffered saline-Tween 20 (TBS-T, 10 mM Tris, 150 mM NaCl, Tween 20 0.1%, pH 7.5) containing non-fat milk (5%) and BSA (3%). After incubation with lipophorin (50 μg/ml), the blots were probed with primary and secondary antibodies as follows: (a) polyclonal anti-lipophorin antibody (1:2000) diluted in TBS-T, (b) HRP-conjugated goat anti-rabbit IgG (secondary antibody; 1:5000) in the same medium. After three washes with TBS, visualization of immunoreaction was performed using the ECL detection kit according to the manufacturer's instructions.

2.6. In-gel trypsin digestion and mass spectrometry analysis

The film obtained from ligand blotting assays was aligned with the Coomassie blue stained gels and lipophorin binding bands were manually excised and further processed according to Martinelli et al. (2014). Briefly, gel pieces were washed, dehydrated, lyophilized and the proteins contained in the gel digested for 16 h at 37 °C (500 μl, in 100 mM ammonium bicarbonate with 10 ng of sequencing grade modified trypsin). After digestion, the samples were lyophilized and submitted to tandem mass spectrometry (MS/MS) analyses in a Liquid Chromatography-Electrospray Ionization-Quadrupole Time of flight (LC-ESI-QTOF) instrument. The material was suspended in 0.1% formic acid (10 μl) and 5 μl were subjected to reversed phase chromatography (NanoAcquity UltraPerformance LC-UPLC, Waters, Milford, United States) using a Nanoease C18, 75 μm ID at 35 °C. The column was equilibrated with 0.1% trifluoroacetic acid (TFA) and the peptides were eluted in a 20 min gradient, ramping from 0 to 60% acetonitrile in 0.1% TFA at 0.6 nL/min constant flow. Eluted peptides were ionized by electro spray process and analyzed by tandem mass spectrometry using a Q-TOF Microspectrometer (Micromass, Waters, Milford, United States). The voltage applied to the cone for the ionization was 35 V. The three most intense ions in the range of m/z 200–2000 and +2 or +3 charges were selected for fragmentation. The acquired MS/MS spectra were processed using Mascot Distiller (2.4.2.0) and search was done using Mascot Daemon (2.3.0) against the INSECTA database (NCBI, taxid:50557, April 2013). The search results were loaded onto Scaffold 3.3.1 for final data analysis. A minimum of two unique peptides, protein probability above 95% and a Mascot score above 30 were considered for a protein hit.

2.7. Immunodetection of β-ATPase in the midgut tissue

The microsomal fraction, enriched in midgut membranes and free of mitochondria, was obtained according to Zalewska et al. (2009). Midgut homogenates in 20 mM Tris–HCl, 150 mM NaCl and 300 mM sucrose were centrifuged to remove cellular debris. Thereafter, the supernatants were centrifuged at 15,000 × *g* (20 min at 4 °C) to pellet the mitochondrial fraction, followed by an ultracentrifugation at 100,000 × *g* (60 min at 4 °C) to obtain the cytosolic and microsomal fractions. Total homogenates and subcellular fractions were subjected to Tris-Tricine electrophoresis as described in section 2.5. The immunodetection of β-ATPase was performed by western blot, using a commercial rabbit anti-β-ATPase antibody (1:1000). Blots were also probed with a commercial rabbit anti-cytochrome *c* antibody (1:1000) to check for mitochondrial contamination of the microsomal fraction.

2.8. Isolation of midgut cells and tissue sectioning

Isolated enterocytes were obtained by the treatment of chopped midguts with collagenase Ia as previously described (Fruttero et al., 2009). Cells were suspended in saline buffer (215 mM NaCl, 4.8 mM KCl, 1 mM $CaCl_2$, 1 mM $MgCl_2$, 5 mM glucose, 40 mM HEPES, pH 7.4) containing 1 mM adenosine 5-monophosphate and 1% BSA. For fixation, midgut cells were dialyzed against 0.05% glutaraldehyde/0.5% formaldehyde in PBS. Cell suspension was stored for one week at 4 °C.

To obtain midgut tissue sections, the dissected organs were fixed in 4% paraformaldehyde in PBS, transferred into sucrose/PBS, embedded in OCT and frozen in liquid nitrogen (Fruttero et al., 2009). Tissue sections of 12 μm were obtained with a Leica CM1510 cryostat (Leica Microsystems, Wetzlar, Germany) and placed onto poly-L-lysine-treated glass slides.

2.9. In vitro binding of lipophorin to β-ATPase in isolated enterocytes

In this approach we first detected the co-localization of lipophorin and β-ATPase in isolated enterocytes by

immunofluorescence assays (termed *in vitro* binding assays). Enterocytes in an appropriate dilution were placed in poly-L-lysine-coated slides and incubated with 1% BSA in PBS for 20 min to block the non-specific binding sites. Then, the slides were sequentially incubated with lipophorin (25 μg/ml) and with the antibodies as follows: anti-β-ATPase (1:100), anti-rabbit IgG labeled with Alexa 568 (1:500) and anti-Lp-FITC (1:80). All incubations were performed in a humid chamber at 37 °C for 1 h and followed by two washes with PBS for 5 min. Nuclei were stained with 300 nM DAPI. Controls were performed without the addition of lipophorin or incubating the enterocytes without either the anti-rabbit IgG labeled with Alexa 568 or the anti-β-ATPase antibody.

To establish the specificity of the *in vitro* lipophorin-β-ATPase binding, slides containing the enterocytes were blocked with an excess of lipophorin (0.5 mg/ml) or with an excess of anti-β-ATPase (1:40) antibody. After the pre-treatments, β-ATPase or lipophorin were detected by standard immunofluorescence assays.

In all cases, coverslips were rinsed with distilled water, air-dried, mounted in Fluorsave and observed with an Olympus FV1000 laser scanning confocal microscope (Olympus, Tokyo, Japan) equipped with 405, 488 and 543 nm lasers. Fluorescence and differential interference contrast (DIC) images were acquired and processed with FluoView FV1000 version 1.7.1.0 software.

2.10. Co-localization of endogenous lipophorin and β-ATPase in the midgut tissue

To detect co-localization of the lipophorin that remains anchored to the midgut *in vivo* (termed "endogenous lipophorin") and β-ATPase, tissue sections were blocked with BSA and then incubated with anti-β-ATPase (1:100). After washing steps, tissue sections were treated with anti-rabbit IgG labeled with Alexa 568 (1:500) and with the anti-Lp-FITC (1:80) and processed for laser confocal microscopy as described in 2.9.

2.11. Co-immunoprecipitation assays

To obtain further evidence of endogenous lipophorin-β-ATPase interaction, the midguts were dissected and then incubated at room temperature with 1.5 mM of the DTSSP crosslinker according to manufacturer's protocol. The reaction was stopped by incubating the organs in 20 mM Tris–HCl pH 8.5 for 15 min. Midguts were processed as described in section 2.7. and the obtained microsomal fraction was incubated with 0.2 μg of anti-β-ATPase antibody (90 min, 4 °C). Afterwards, 50 μl of reconstituted protein A-Sepharose was added and incubated overnight at 4 °C, with gentle agitation. The immunoprecipitate was isolated by centrifugation and washed several times with 1% IGEPAL CA-630 in PBS. The proteins bound to the beads were eluted with SDS sample buffer (Laemmli, 1970) and protein A-Sepharose was removed by centrifugation. Controls incubating the microsomal fraction (input) without anti-β-ATPase antibody or with anti-BSA antibody, an irrelevant antibody, were performed. The eluted proteins, the input and lipophorin were subjected to western blot as described in section 2.7, and probed against the anti-lipophorin antibody.

2.12. The effect of in vivo β-ATPase blocking on lipid transfer from the midgut to the hemolymph

The insects were fed individually using an artificial feeder with a mixture of hen blood and 1% BSA in PBS (1:1 v/v) containing [9,10-^{3}H]-oleic acid (~1 μCi/insect). Five hours after artificial feeding the insects were injected with 10 μg of either, an anti-β-ATPase antibody or anti-BSA antibody (control). The antibodies were previously dialyzed against PBS. As an additional control, a group of insects were injected with PBS. In all cases, after 1 h of injection, the hemolymph was individually collected in disposable micro-glass tubes and subjected to radioactivity counting in a Wallac 1214 Rackbeta liquid scintillation counter (PerkinElmer Wallac Oy, Turku, Finland).

In another set of experiments, the hemolymph pools collected from insects fed with [9,10-^{3}H]-oleic acid and injected with the anti-β-ATPase or anti-BSA antibodies as indicated above were processed for lipid extraction (Folch et al., 1957) or subjected to KBr gradient ultracentrifugation for lipophorin isolation (Fruttero et al., 2009). Extracted lipids were dried under N_2 and separated by thin-layer chromatography (TLC) on silica gel using hexane-ethyl ether-formic acid 70:30:3 (v/v/v) as a solvent system. Lipid fractions were visualized with iodine vapor, scraped from the plates, and radioactivity was determined for each fraction.

2.13. The effect of in vivo β-ATPase blocking on lipid transfer from lipophorin to the midgut

For this set of studies, insects kept at 28 °C were injected with 5 μl of anti-β-ATPase antibody dialyzed against PBS (10 μg/insect). Thirty minutes post-injection, insects were treated as follows: a) injected with 5 μl of Lp-DiI (10 μg/insect) and dissected 15 min later; b) injected with 5 μl of Lp-Bodipy-FA (10 μg/insect) and dissected 60 min later. The midguts were processed for cryostat sectioning and analyzed by laser confocal microscopy as described in 2.9. Insects were also injected with PBS or with anti-BSA as controls. In addition, Bodipy-FA transferred to the midgut was estimated after dissected tissues were weighed and subjected to lipid extraction (Folch et al., 1957), using the Multi-Mode Microplate Reader Sinergy HT (BioTek Instruments, Winooski, VT, USA) with 485–505/528-548 nm excitation/emission filters. Results were expressed as arbitrary units of fluorescence/mg of tissue.

2.14. Fluorescence quantification

The relative intensity of fluorescence from laser confocal microscopy images was determined by establishing the mean grey value of pixels in manually defined areas of the plasma membrane using ImageJ software. The background was subtracted by taking a representative area as reference using the plugin "BG subtraction from ROI". The quantification was performed using 5 regions of interest (ROIs) per cell of 10 × 10 pixels in sectors of maximum intensity of the plasma membrane. The threshold for the signal was established considering the fluorescence detected in the control experiments. Three different experiments were performed and the digital data of 50 individual cells for each treatment was recorded.

2.15. Statistical analysis

In the approaches directed to analyze the effect of *in vivo* β-ATPase blocking on lipid transfer from the midgut to the hemolymph, data from the insects (n = 8–10 per condition) were analyzed using One-way parametric ANOVA for comparisons. For the experiments in which the transfer of lipids from lipophorin to the midgut was analyzed, insects were processed individually ($n = 5$) and the Bodipy-FA fluorescence in midgut lipid extracts was recorded by duplicate. One-way parametric (for fluorescence of extracted lipids) or nonparametric ANOVA (for enterocyte fluorescence) was used for comparisons. In all cases, graphs and statistical tests were performed using GraphPad Prism 5 and GraphPad Instat 3.0 computer programs. Unless otherwise stated, results were expressed as mean ± SEM and a P value <0.05 was considered statistically significant.

3. Results

3.1. Characterization of lipophorin binding proteins at the midgut membrane

To characterize and identify the lipophorin binding proteins at the midgut membrane of fifth instar nymphs of *P. megistus*, a combination of ligand blotting assays and tandem mass spectrometry was used. The ligand blotting showed the presence of two main lipophorin binding fractions of 56 and 48 kDa (Fig. 1A, lane 3) that were absent in the control lane (Fig. 1A, lane 2). When the ligand blotting films were aligned with the electrophoretic gels and the corresponding bands were excised, in-gel digested with trypsin and processed for MS/MS analysis (Fig. 1B), the 56 kDa fraction retrieved the β-ATPase from *Tribolium castaneum*. In addition, for the 48 kDa fraction the match corresponded to actin 5C from *D. melanogaster*. Three independent samples from different membrane preparations gave the same set of results when searched against the NCBI database. A weak binding fraction of 60 kDa was also detected in the ligand blotting assay and identified as α-ATPase from *Aedes aegypti* (data not shown).

Taking into account that the presence of β-ATPase in the plasma membrane of different cell types has been extensively documented (Chi and Pizzo, 2006; Vantourout et al., 2010) and that it has been reported as a receptor of the High-Density Lipoprotein (HDL) (Martinez et al., 2003), we focused the study in the characterization of the role of the β-ATPase as a lipophorin binding protein in the midgut membrane as well as on its involvement in the transfer of lipids.

To further confirm the identity of the β-ATPase, primers were designed based on the partial amino acid sequence of peptides obtained from MS/MS and from the β-ATPase nucleotide sequences of related species. A single PCR product of the expected size and sequence was amplified (Supplementary Fig. 1A–B). When a BLAST analysis was performed (Basic Local Alignment Search Tool; Altschul et al., 1990) using the default setting, the best match retrieved (84% identity) was the β-ATPase from the hemipteran *Rhopalosiphum padi* (GenBank: AJ296765).

The sequence of the β-ATPase is evolutionary well conserved. It displays a high percentage of identity between the deduced amino acid sequence of the PCR fragment of the putative β-ATPase from *P. megistus* and its counterpart from humans (100%). These facts allowed us to employ a commercial polyclonal anti-β-ATPase antibody of human origin for further experiments.

3.2. β-ATPase in the plasma membrane of the midgut

To obtain evidence about the localization of the β-ATPase, the microsomal fraction enriched in midgut membranes and free of mitochondria as well as other subcellular midgut fractions were

(A)

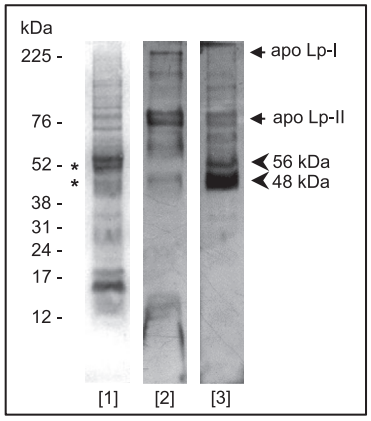

(B)

Accesion # (NCBI)	Protein name	Mascot score	Observed MW	Unique peptides	Sequence coverage (%)
283046836	ATP synthase subunit beta, Mitochondrial (*Tribolium castaneum*)	31	56 kDa	AHGGYSVFAGVGER AIAELGIYPAVDPLDSTSR DQEGQDVLLFIDNIFR FTQAGSEVSALLGR IINVIGEPIDER LVLEVAQHLGENTVR TIAMDGTEGLVR TVLIMELINNVAK VALTGLTVAEYFR VALVYGQMNEPPGAR	55.28
17530805	Actin 5C, Isoform B (*Drosophila melanogaster*)	30	48 kDa	AVFPSIVGRPR DLYANTVLSGGTTMYPGIADR DSYVGDEAQSKR IWHHTFYNELR LCYVALDFEQEMATAASSSSLEK SYELPDGQVITIGNER	41.82

Fig. 1. Identification of lipophorin binding proteins by ligand blotting and tandem mass spectrometry (MS/MS). **(A)**, Midgut membrane proteins (30 μg) were subjected to electrophoresis under non-denaturing conditions (lane 1, stained with Coomassie Brilliant Blue), transferred to nitrocellulose and blocked. The nitrocellulose membranes were incubated with the anti-lipophorin antibody (control, lane 2) or with lipophorin (50 μg/ml) and then with the anti-lipophorin antibody (lane 3). Arrows indicate apolipophorin I and II (apoLp-I and apoLp-II) while arrowheads indicate two lipophorin binding bands, which are absent in the control. Molecular weight markers are shown on the left of the panel. **(B)**, MS/MS identification of lipophorin binding proteins. The corresponding bands in lane 1 of (A) (asterisks) were excised from the gels and identified by LC-ESI-QTOF. The results were searched against using the INSECTA database (NCBI).

probed against the anti-β-ATPase antibody by western blot (Fig. 2A). The commercial anti-β-ATPase antibody recognized a band of 56 kDa compatible with β-ATPase in the total midgut homogenate and, as expected, in the mitochondrial fraction. However, β-ATPase was also immunodetected in the microsomal fraction, strongly suggesting its localization in the plasma membrane. Densitometric estimations indicated that about 73% of β-ATPase signal was mitochondrial and that 27% was found in membranes (results not shown). To rule out mitochondrial contamination of the microsomal fraction, this sample was also tested with an antibody directed to cytochrome *c*. As shown in the Fig. 2B, no signal for this mitochondrial marker was found in the membrane preparations.

3.3. The binding of lipophorin to β-ATPase in isolated enterocytes

The co-localization of lipophorin and β-ATPase was evidenced by immunofluorescence assays on isolated enterocytes and in the presence of added lipophorin. Under this condition, anti-Lp-FITC showed that lipophorin was found in the basolateral membrane of the enterocyte (Fig. 3B), a region that is in contact with the hemolymph. When the control experiments were performed without the addition of lipophorin, no significant fluorescence was observed probably due to the removal of endogenously bound lipophorin by collagenase treatment (result not shown). On the other hand, β-ATPase was detected at the plasma membrane of non-permeabilized enterocytes (Fig. 3A), in agreement with the results from the subcellular fractioning. Moreover, it was shown that lipophorin and β-ATPase partially co-localized at the basolateral region of the enterocytes, supporting the binding of both proteins (Fig. 3D).

To establish the specificity of the lipophorin-β-ATPase binding, immunofluorescence assays were performed with a 20-fold excess lipophorin (Fig. 4C), which in turn would block the subsequent binding of the anti-β-ATPase antibody and decrease the fluorescent red signal for β-ATPase/Alexa 546 in the enterocytes. Control experiments were made by pre-incubating the enterocytes with PBS (Fig. 4A) or with 25 μg/ml of lipophorin (Fig. 4B). As shown by the fluorescence quantification (Fig. 4D), the excess of lipophorin significantly reduced the immunoreactivity of the anti-β-ATPase antibody ($P < 0.001$).

The reciprocal immunofluorescence assay, aimed to block the binding of the added lipophorin to the enterocytes was performed by pre-incubating the cells with an excess of anti-β-ATPase antibody (Fig. 4G). Controls were performed by pre-incubating the enterocytes with PBS or with anti-BSA antibody (Fig. 4E–F). Fluorescence quantification showed that the excess of anti-β-ATPase antibody significantly reduced the immunoreactivity for the anti-Lp-FITC antibody (Fig. 4H; $P < 0.001$). Taken together, this set of results confirmed the specificity of the binding between lipophorin and β-ATPase at the plasma membrane of isolated enterocytes.

3.4. The interaction of the endogenous lipophorin and β-ATPase

Whereas ligand blotting and immunofluorescence assays with isolated enterocytes demonstrated the binding of lipophorin and β-ATPase *in vitro*, the co-immunoprecipitation approach evidenced the interaction between the endogenous lipophorin, which remains anchored to cell membranes *in vivo,* and β-ATPase. Results showed that endogenous lipophorin present in the microsomal fraction co-immunoprecipitated with the anti-β-ATPase antibody (Fig. 5, lane IP), while the use of an irrelevant antibody (anti-BSA) did not retrieve any non-specifically immunoprecipitated lipophorin (Fig. 5, lane control). The presence of endogenous lipophorin in the microsomal fraction was confirmed by the signal in the "input" lane (Fig. 5).

Further evidence in support of the *in vivo* binding between the endogenous lipophorin and β-ATPase was obtained by performing immunofluorescence assays employing non-permeabilized midgut tissue sections. It was shown that the signal for the β-ATPase was distributed mainly at the apical and basal regions of the tissue (Fig. 6B). However, the fluorescence for endogenous lipophorin was restricted to the sub-epithelial layer of the midgut tissue, partially co-localizing with the β-ATPase in focalized areas, thus confirming their binding (Fig. 6C–D).

3.5. The effect of β-ATPase blocking on lipid transfer from the midgut to the hemolymph

It was previously demonstrated that in *P. megistus*, ingested triacylglycerol is hydrolyzed to fatty acids in the midgut lumen, fatty acids are in turn absorbed by the enterocytes, used in the synthesis of neutral lipids and exported to circulating lipophorin as diacylglycerol (Canavoso et al., 2004a). Therefore, to test whether blocking the β-ATPase would interfere on the lipid transfer from the midgut to lipophorin, insects were fed with [^{3}H]-oleic acid and then injected with the anti-β-ATPase antibody or the anti-BSA-antibody (control).

In [^{3}H]-oleic acid-fed insects, the transfer of radiolabeled lipids from the midgut to the hemolymph, mainly diacylglycerol, increased at a nearly constant rate between 2.5 and 10 h post-feeding (Fig. 7A). Injections of anti-β-ATPase or anti-BSA were performed 5 h post- feeding. As shown in Fig. 7B, 1 h after blocking the β-ATPase with the anti-β-ATPase antibody, the transfer of [^{3}H]-labeled lipids to the hemolymph was significantly reduced in 42% when compared to insects injected with PBS or anti-BSA antibody ($P < 0.01$). As expected, in the hemolymph more than 80% of the label was found as diacylglycerol in insects injected with the anti-β-ATPase antibody and controls (Fig. 7C). Moreover, in all cases, [^{3}H]-diacylglycerol was associated to lipophorin (results not shown).

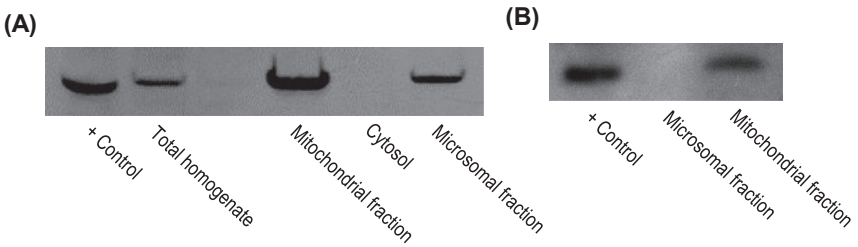

Fig. 2. Immunodetection of β-chain of ATP synthase (β-ATPase) in the midgut tissue. **(A)**, Midguts were homogenized and processed as stated in Materials and Methods to obtain the cytosolic and microsomal fractions. Subcellular fractions were probed with a polyclonal anti-β-ATPase antibody. Approximately 40 μg of proteins were loaded into each lane. **(B)**, Subcellular fractions were probed with a polyclonal anti-cytochrome *c* antibody to evaluate mitochondrial contamination of microsomal fraction. In (A) and (B), a homogenate of rat brain was used as positive control for β-ATPase and cytochrome *c*.

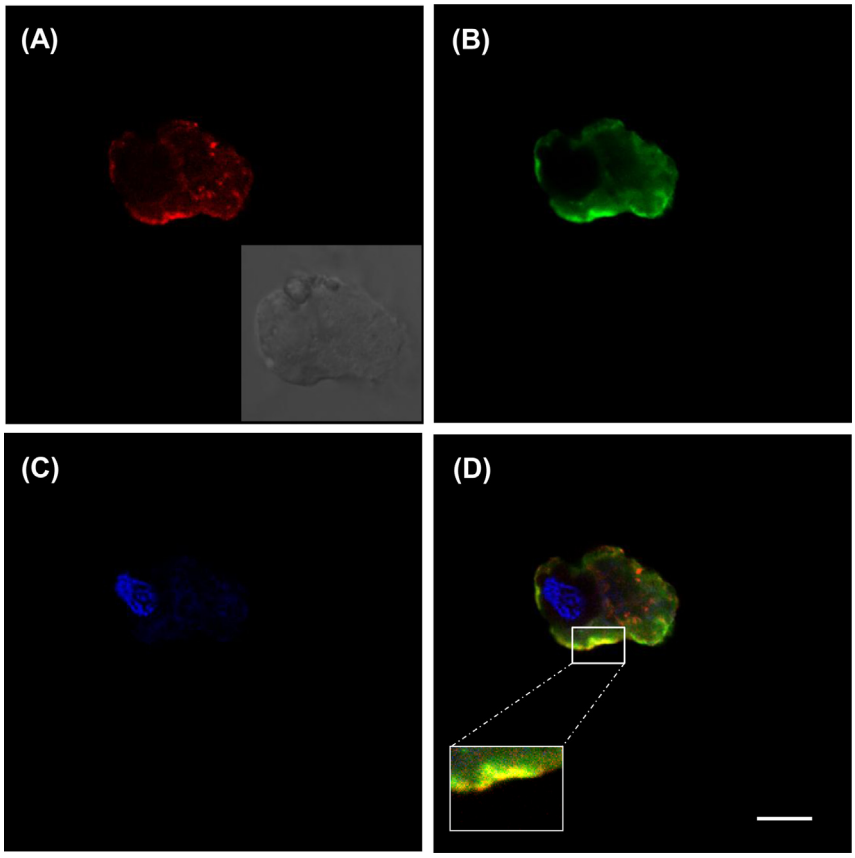

Fig. 3. Localization of lipophorin and the β-chain of the ATP synthase (β-ATPase) in enterocytes of *P. megistus* by immunofluorescence assays. After isolation from the midgut by collagenase treatment, enterocytes were incubated with lipophorin (25 μg/ml), anti-β-ATPase, anti-IgG labeled with Alexa 568 and anti-Lp-FITC as stated in Materials and Methods. Nuclei were stained with DAPI **(C)**. **(A–B)**, Fluorescence distribution of β-ATPase (red) and lipophorin (green), respectively. Insert in (A) shows the corresponding DIC image. **(D)**, Merged image of (A–C). The insert shows the area indicated in the box, at higher magnification. Bar: 15 μm. (For interpretation of the references to colour in this figure legend, the reader is referred to the web version of this article.)

3.6. The effect of β-ATPase blocking on lipid transfer to the midgut

This approach was carried out to analyze if blocking the β-ATPase would also impair lipophorin-mediated lipid transfer to the midgut tissue, a less important route of lipid delivery to this tissue. When the anti-β-ATPase antibody was injected into the hemocoel of the insects and 30 min later, Lp-DiI was injected to follow the fate of the entire particle, the binding of Lp-DiI to the sub-epithelial layer of the midgut tissue was impaired when compared with the fluorescence found in control insects (Fig. 8A–B). In addition, control experiments demonstrated that the injected anti-β-ATPase antibody was located at the sub-epithelial areas of midgut tissue (Supplementary Fig. 2). Furthermore, when anti-β-ATPase treated insects were injected with Lp-Bodipy-FA to follow the lipoprotein lipid cargo, a remarkable decrease in the signal for Bodipy-FA was observed in the lipid droplets when compared to the insects injected with the anti-BSA antibody (Fig. 8C–D). The effect of the anti-β-ATPase antibody on fatty acid transfer to the midgut was also evident as a decreased signal of Bodipy-FA fluorescence found in the tissue after lipid extraction (Fig. 8E, $P < 0.05$ vs. insect controls injected with PBS or anti-BSA antibody).

4. Discussion

Although the "reusable shuttle" paradigm of lipophorin function was proposed several decades ago, there are aspects of its functioning that remain to be elucidated (Chino et al., 1977). It has been suggested that lipophorin lipid transfer at the cell membrane is selective, implying that several molecular actors must be participating in the process (Arrese et al., 2001). Currently, there are few characterized candidates supporting the functioning and selectivity of the docking mechanism of lipophorin-mediated lipid transfer. It has been shown that the two isoforms of lipophorin receptors from *D. melanogaster* Lpr1 and Lpr2, which are related to the mammalian LDL receptor, mediate the uptake of neutral lipids in oocytes and imaginal disc cells by favoring the extracellular lipolysis of lipophorin (Parra-Peralbo and Culi, 2011). Nevertheless, it is unclear to what extent these receptors affect the rate of exchange of neutral lipids to other tissues since lipid content in fat body and hemolymph found in knockout and wild type receptor flies did not show significant differences. On the other hand, the transmembrane proteins expressed in the silk gland of *B. mori*, Cameo2 and SCRB15, seem to function as non-endocytic lipophorin receptors that facilitate the selective uptake of carotenoids. However, the role of CD36 family members in the transfer of neutral lipids, the major lipid class carried by lipophorin, remains elusive (Sakudoh et al., 2013).

We have previously demonstrated the presence of lipophorin binding sites in the midgut membranes of the hematophagous insect *P. megistus* and characterized the properties of this interaction (Fruttero et al., 2009). Moreover, the lack of an endocytic pathway for lipophorin in the midgut was also demonstrated by *in vivo* assays (Fruttero et al., 2009). Taking into account that there is no availability of cell culture, mutants or sequenced genome of *P. megistus*, the combination of ligand blotting assays and mass spectrometry analysis allowed us to identify the β-ATPase and actin as midgut membrane proteins able to bind lipophorin, which in

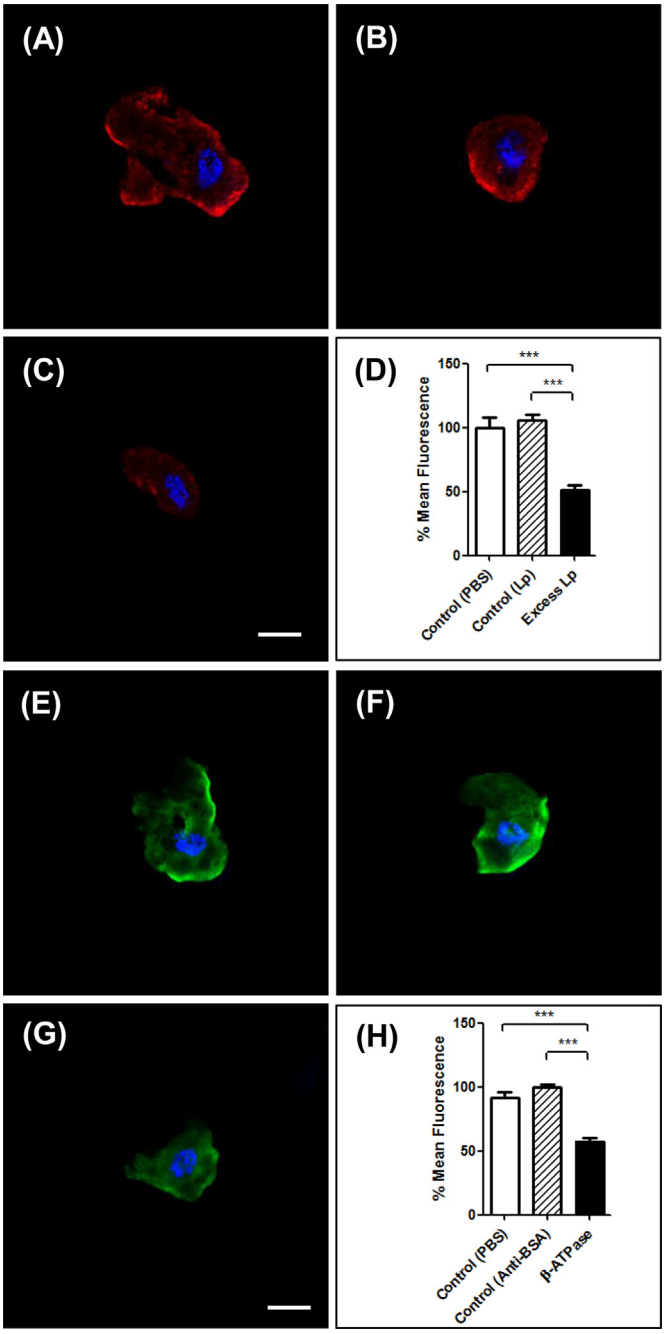

Fig. 4. The specificity of lipophorin-β-chain of ATP synthase (β-ATPase) binding in isolated enterocytes. **(A–C)**, Cells were incubated with PBS (control, A), with 25 μg/ml of lipophorin (control, B), or with a 20-fold excess of lipophorin (C), before the incubation steps with the antibodies anti-β-ATPase and anti-IgG labeled with Alexa 568 as stated in Material and Methods. **(D)**, Quantification of the relative red fluorescence in sections of the plasma membrane of enterocytes corresponding to (A–C) treatments. ***, $P < 0.001$. **(E–G)**, Cells were incubated with PBS (control, E), with 5 ng/μl of an irrelevant antibody (anti-BSA, control, F), or with 5 ng/μl (1:40) of anti-β-ATPase antibody (G), before the incubations with anti-Lp-FITC. **(H)**, Quantification of the relative green fluorescence in sections of the plasma membrane of enterocytes corresponding to (E–G) treatments. ***, $P < 0.001$. In all cases, nuclei were stained with DAPI. Bars: 15 μm. (For interpretation of the references to colour in this figure legend, the reader is referred to the web version of this article.)

turn would function as non-endocytic receptors. In agreement with this finding, we have previously reported two lipophorin binding fractions in the midgut with molecular weights close to those reported for β-ATPase and actin (Fruttero et al., 2009).

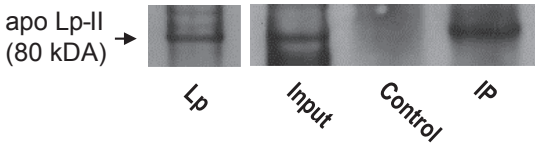

Fig. 5. Co-immunoprecipitation of endogenous lipophorin (Lp) and β-chain of ATP synthase (β-ATPase). Microsomal fractions of the midguts (60 μg, Input) obtained as stated in Materials and Methods were incubated with 0.2 μg of anti-BSA antibody (Control) or with 0.2 μg of anti-β-ATPase antibody (IP). Samples were transferred to nitrocellulose and then probed against anti-lipophorin antibody. In all lines, the presence of lipophorin (visualized as apo Lp-II) is indicated with an arrow. IP lane, co-immunoprecipitation of lipophorin with the anti-β-ATPase antibody; Input lane, endogenous lipophorin; Lp line, purified lipophorin loaded as a reference.

Actin is a cytoplasmic protein and, taking into account that lipophorin is not taken up by the midgut cell (Fruttero et al., 2009), the physiological relevance of a lipophorin-actin interaction is currently unknown. However, the presence of actin in membrane preparations is not surprising, because its occurrence in brush border membrane vesicles of *Heliothis virescens,* where it was identified as a Cry1Ac-binding protein, was already reported (Krishnamoorthy et al., 2007) .

Several functions are attributed to the cell surface ATPase complex in mammals, including lymphocyte-mediated tumor cell cytotoxicity, cell survival, tumor recognition, food intake and synaptic plasticity regulation, among others (Chi and Pizzo, 2006; Vantourout et al., 2010). There are also roles attributed to the complex in invertebrates. In this context, Zalewska et al. (2009) showed that the α and β subunits of the ATPase complex present in the plasma membrane of fat body cells of *G. mellonella* can bind the juvenile hormone binding protein (JHBP), thus participating in the control of the endocrine system of this species.

The most thoroughly understood function of the cell surface β-ATPase is that of endocytic receptor during hepatic HDL-cholesterol uptake (Martinez et al., 2003, 2004; Röhrl and Stangl, 2013). Taking into account that lipophorin is a high-density lipoprotein together with the fact that cell surface β-ATPase has been reported in insects (Zalewska et al., 2009; Galetto et al., 2011), the interaction lipoprotein-β-ATPase is of particular relevance in the context of our findings. To play a role as a lipophorin receptor, the β-ATPase must be located in the plasma membrane of the cell. In *P. megistus* we showed by RT-PCR and western blot that β-ATPase is expressed in the midgut cells. Moreover, it was shown that β-ATPase co-localizes with lipophorin in the basal region of the plasma membrane of isolated enterocytes, supporting the interaction between both proteins. In agreement with our results, several reports described the presence of various subunits of ATPase in the surface of the cell. In some cases, it has been determined that the whole and fully functional ATPase complex is in caveolae or lipid rafts (Vantourout et al., 2010).

Similar to vertebrates, the cell surface ATPase complex in invertebrates seems to be involved in different physiological roles depending of the ligand and the cell type. The combination of affinity chromatography and mass spectrometry allow demonstration of the binding of the major phytoplasma antigenic membrane protein, Amp, with the ATPase of the midgut and salivary glands of phloem-sucking hemipteran insects. Such an interaction seems to regulate the insect transmission specificity (Galetto et al., 2011). The ATPase complex of the crayfish *Pacifastacus leniusculus* acts as the receptor of the cytokine astakine, thus participating in the hematopoietic process (Lin et al., 2009). In the sucking-blood *P. megistus,* the binding of anti-β-ATPase antibody or lipophorin to the surface of enterocytes was significantly blocked by an excess of lipophorin or anti-β-ATPase antibody, respectively, evidencing

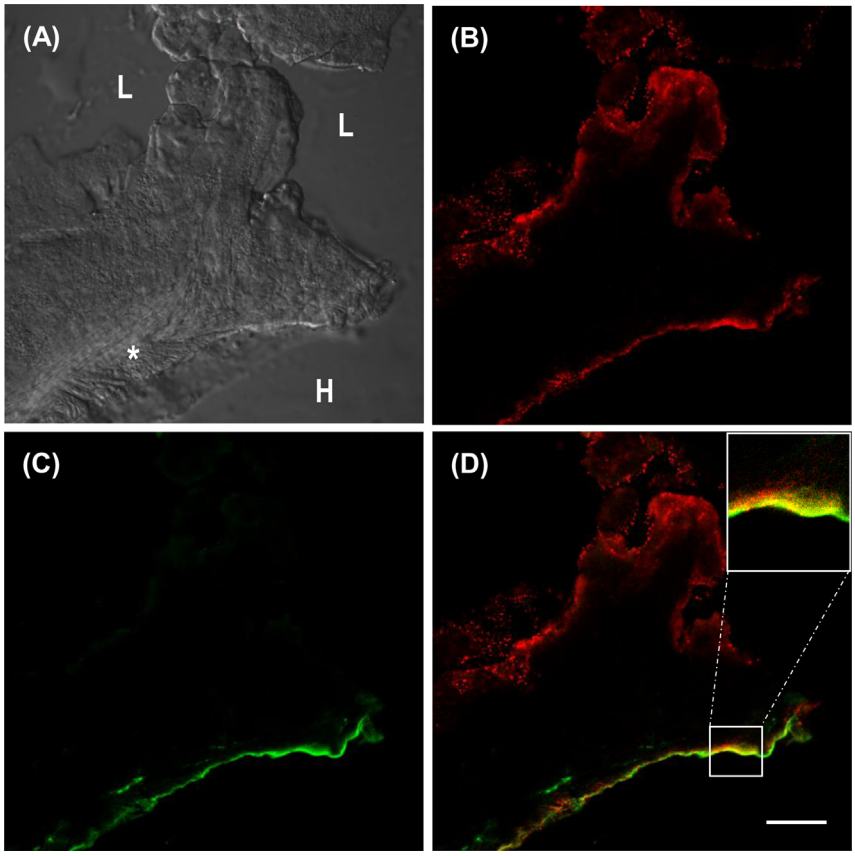

Fig. 6. Localization of the β-chain of ATP synthase (β-ATPase) and endogenous lipophorin in the midgut tissue. Cryostat tissue sections were incubated with the antibodies anti-β-ATPase, anti-IgG labeled with Alexa 568 and anti-Lp-FITC as stated in Materials and Methods. **(A)**, DIC image of the tissue. **(B–C)**, The fluorescence pattern corresponding to the β-ATPase (red) and lipophorin (green), respectively. **(D)**, Merged image of (B) and (C) showing the partial co-localization of lipophorin and β-ATPase. The insert shows the area indicated in the box at higher magnification. H, hemolymph; L, lumen, asterisk: sub-epithelial layer of the midgut tissue. Bar: 10 μm. (For interpretation of the references to colour in this figure legend, the reader is referred to the web version of this article.)

the specificity of β-ATPase-lipophorin binding. Supported by the well documented fact that lipophorin remains anchored to the cell membrane preparations even after extensive removal treatments (Canavoso et al., 2004b; Fruttero et al., 2009), we obtained further evidences of the *in vivo* β-ATPase-endogenous lipophorin interaction. Both molecules were co-immunoprecipitated from midgut membranes and partially co-localized in the midgut tissue. Using immortalized human hepatocytes, Martinez et al. (2003)

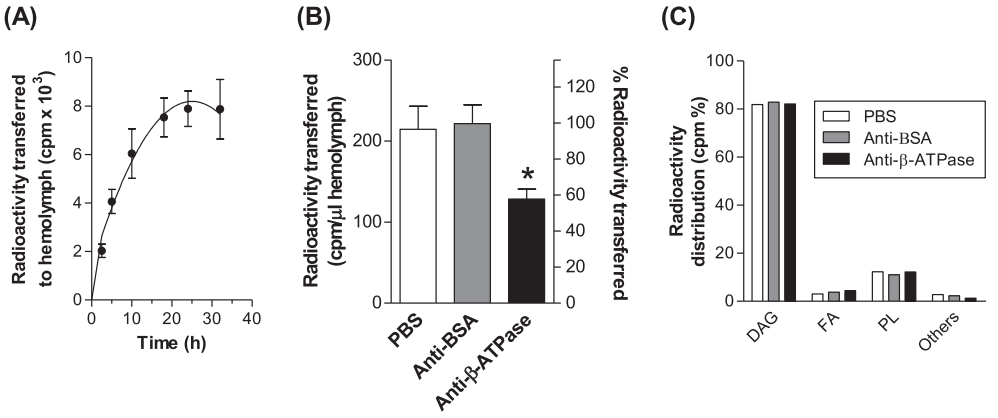

Fig. 7. The effect of blocking the β-chain ATP synthase (β-ATPase) on lipid transfer from midgut to lipophorin. **(A),** Time course of radioactivity transfer from labeled midgut to the hemolymph. The insects were fed with [^{3}H]-oleic acid and at different times, the hemolymph was individually collected and subjected to radioactivity counting. The results are expressed as total cpm ± SEM. **(B),** The insects were fed with [^{3}H]-oleic acid and 5 h later injected with PBS (control), an irrelevant antibody (anti-BSA, control) or anti-β-ATPase antibody as stated in Materials and Methods. One hour post-injection the hemolymph was collected, the volume measured and the associated radioactivity counted. The results are expressed as cpm/μl of hemolymph ± SEM and as % of radioactivity transferred to hemolymph ± SEM. *, $P < 0.01$ vs. controls. **(C),** The insects were treated as in (B) and the collected hemolymph was subjected to lipid extraction. Lipid extracts were separated by TLC and the radioactivity in each fraction determined by liquid scintillation assay of silica gel scrapings. The results are expressed as radioactivity distribution (cpm %) and one representative experiment is shown. DAG, diacylglycerol; FA, fatty acids; PL, phospholipids.

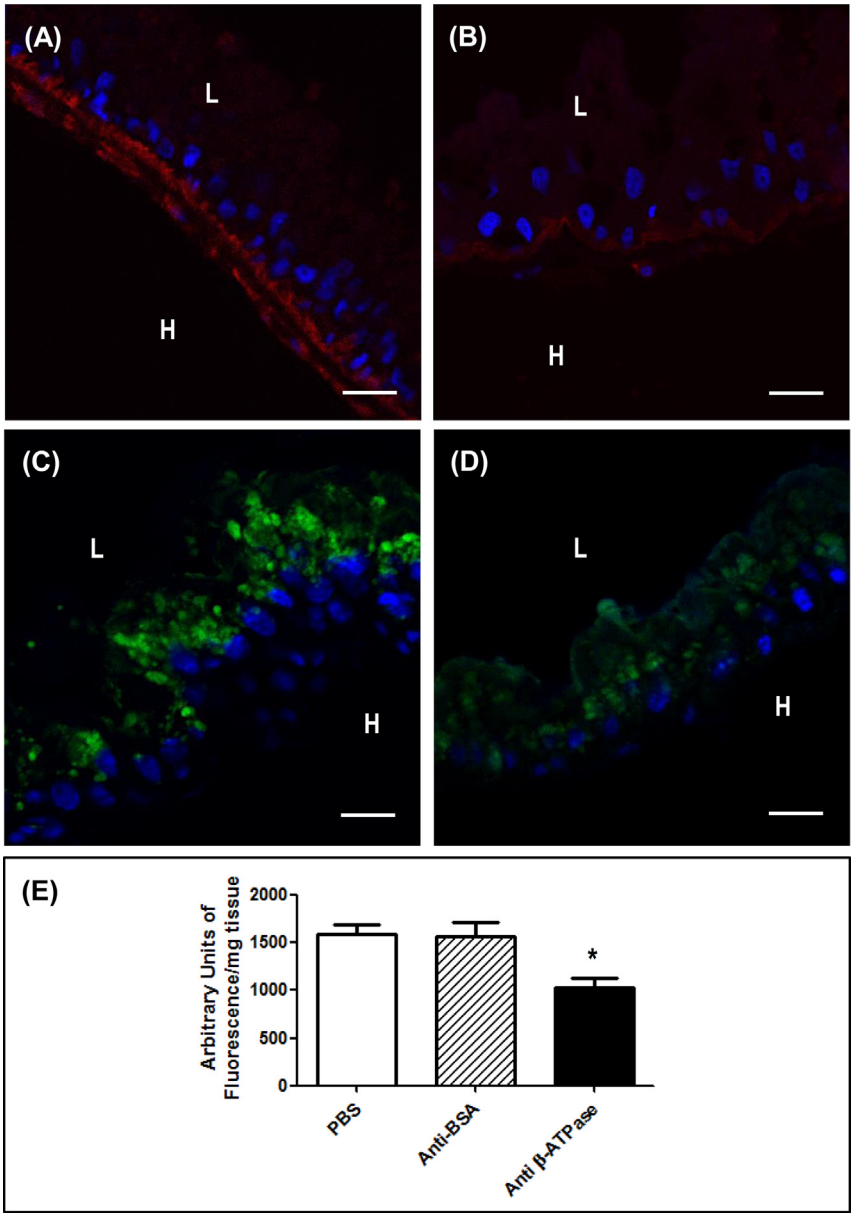

Fig. 8. The effect of β-chain of ATP synthase (β-ATPase) blocking on lipophorin lipid transfer to the midgut. The insects were injected with either, an irrelevant antibody (anti-BSA, control) or anti-β-ATPase antibody as stated in Materials and Methods. Thereafter, the insects were injected with Lp-DiI to trace the lipophorin particle and dissected 15 min later. Anti-BSA or anti-β-ATPase treated insects were injected with Lp-Bodipy-FA to follow the lipophorin lipid cargo and dissected 60 min later. Midguts were fixed and processed for confocal laser microscopy. **(A and C)**, Tissue sections of insect controls treated with anti-BSA antibody followed by Lp-DiI (A, red) or Lp-Bodipy-FA (C, green) injection. **(B and D)**, Midgut tissue sections corresponding to insects treated with the anti-β-ATPase antibody followed by Lp-DiI (B) or Lp-Bodipy-FA (D) injection. The nuclei were stained with DAPI. H, hemolymph; L, lumen. Bars: 15 μm. **(E)**, Bodipy-FA fluorescence quantification. Total lipids of control insects injected with PBS followed by Lp-Bodipy-FA injection (PBS) or treated as in (C–D) (anti-BSA and anti-β-ATPase, respectively) were extracted and the fluorescence measured and expressed in arbitrary units. $^{*}P < 0.05$ vs. insect injected with PBS or with anti-BSA antibody. (For interpretation of the references to colour in this figure legend, the reader is referred to the web version of this article.)

demonstrated that β-ATPase co-localized with Apo A-I, the main HDL apoprotein, at the surface of the cell. It was also shown that the interaction β-ATPase-Apo A-I promotes the endocytosis of the whole and fully lipidated HDL and involves an increase of the cell surface ATPase hydrolase activity and the activation of a purinergic $P2Y_{13}$ receptor (Martinez et al., 2003; Jacquet et al., 2005). However, reports of the cell surface ATP synthase activity are controversial (Vantourout et al., 2010). Although ATPase activity has not been investigated in the midgut membranes of *P. megistus*, several lines of evidence in mammals (Vantourout et al., 2010) seem to rule out the physiological relevance of the enzymatic activity of the complex in the ATPase-lipophorin interaction. Additional experiments will be needed to address if the ATPase activity is involved in the lipid transfer and/or in lipophorin shuttle mechanism.

From a physiological viewpoint, *in vivo* functional studies showed that the transfer of radiolabeled lipids, mainly diacylglycerol, from the midgut to the hemolymph was significantly impaired by the anti-β-ATPase antibody injection. The relevance of this finding resides in the fact that the blocking of β-ATPase interferes with diacylglycerol export from midgut, one of the most relevant functions of this organ in the context of lipid metabolism (Canavoso et al., 2001). In addition, injecting the anti-β-ATPase antibody in the hemocoel of the insects not only significantly

blocked the binding of lipophorin to its binding sites at the subepithelial layer of the midgut but also, partially impaired the transfer of fatty acid from lipophorin to the midgut. Although the transfer of fatty acids from lipophorin to the midgut has a limited physiological relevance, such a process has been previously reported in *Rhodnius prolixus* and seems to be of significance in starvation conditions (Atella et al., 2000). In addition, in fifth instar nymphs of *P. megistus,* we demonstrated that the binding of lipophorin to the midgut is reversible, facilitating lipid loading and uploading at the tissue (Fruttero et al., 2009).

It is worthy of note that in the present work, α-ATPase was also identified as a midgut protein that can weakly bind lipophorin. In *D. melanogaster*, the α-ATPase subunit was reported as a lipophorin binding protein, as shown by the two-hybrid assay (Giot et al., 2003), suggesting that this interaction could be relevant in *P. megistus*; i. e. α-ATPase can collaborate with β-ATPase in lipophorin binding. Taking into account that these subunits do not possess any membrane-anchoring domain, it is expected their location in the membrane as part of the whole ATPase complex.

In summary, the results presented in this work strongly suggests that cell surface β-ATPase, most likely as part of the F_1F_O ATPase complex, plays a role as a docking receptor of lipophorin in the midgut of *P. megistus*. Currently, it is unknown whether β-ATPase may act in concert with other factors such as lipoprotein lipase, lipid transfer particle (LTP) or integral membrane proteins thus contributing to the transfer of lipid at the cell surface. Taking into account that lipid transfer at the plasma membrane is highly selective (Sakudoh et al., 2010, 2013; Parra-Peralbo and Culi, 2011), it is expected that more than one type of lipophorin receptor can be operating depending on the species, the cell type or tissue as well as the metabolic insect status. The unique properties of lipophorin-mediated lipid transfer in insects advices caution in assigning new binding partners to lipophorin, being necessary more studies to fully understand the mechanism involving the cell surface β-ATPase in such a process. However, the fact that blocking the β-ATPase significantly impairs lipid transfer from the midgut to circulating lipophorin points out that its function must be of physiological relevance.

Acknowledgments

This work was supported by grants from CONICET (PIP 2011–2013), SECyT-Universidad Nacional de Córdoba, Ministerio de Ciencia y Tecnología de Córdoba (PID 2010-MINCyT), and by the Argentine/Brazilian SPU-CAPES Program for graduate students. C.R.C. acknowledges financial support from the Brazilian agencies CAPES, CNPq (PROSUL 490090/2010-9 Ed. 08/2010) and FAPERGS. The authors are grateful to R. Stariolo (Coordinación Nacional de Control de Vectores, Córdoba, Argentina) for help in insect rearing and to Dr. B. Settembrini for critical reading of the manuscript.

Appendix A. Supplementary data

Supplementary data related to this article can be found at http://dx.doi.org/10.1016/j.ibmb.2014.06.002.

References

Altschul, S.F., Gish, W., Miller, W., Myers, E.W., Lipman, D.J., 1990. Basic local alignment search tool. J. Mol. Biol. 215, 403–410.
Andries, K., Verhasselt, P., Guillemont, J., Göhlmann, H.W., Neefs, J.M., Winkler, H., Van Gestel, J., Timmerman, P., Zhu, M., Lee, E., 2005. A diarylquinoline drug active on the ATP synthase of *Mycobacterium tuberculosis*. Science 307, 223–227.
Arechaga, I., Jones, P.C., 2001. Quick guide: ATP synthase. Curr. Biol. 11, R117.
Arrese, E.L., Canavoso, L.E., Jouni, Z.E., Pennington, J.E., Tsuchida, K., Wells, M.A., 2001. Lipid storage and mobilization in insects: current status and future directions. Insect Biochem. Mol. Biol. 31, 7–17.
Atella, G.C., Arruda, M.A., Masuda, H., Gondim, K.C., 2000. Fatty acid incorporation by *Rhodnius prolixus* midgut. Arch. Insect Biochem. Physiol. 43, 99–107.
Bauerfeind, R., Komnick, H., 1992. Lipid loading and unloading of lipophorin in the midgut epithelium of dragonfly larvae (*Aeshna cyanea*): a biochemical and immunocytochemical study. J. Insect Physiol. 38, 147–160.
Bradford, M.M., 1976. A rapid and sensitive method for the quantitation of micrograms quantities of protein utilizing the principle of protein-dye binding. Anal. Biochem 72, 248–254.
Canavoso, L.E., Rubiolo, E.R., 1995. Interconversions of lipophorin particles by adipokinetic hormone in hemolymph of *Panstrongylus megistus, Dipetalogaster maximus* and *Triatoma infestans* (Hemiptera: Reduviidae). Comp. Biochem. Physiol. 112A, 143–150.
Canavoso, L.E., Jouni, Z.E., Karnas, J.K., Pennington, J.E., Wells, M.A., 2001. Fat metabolism in insects. Annu. Rev. Nutr. 21, 23–46.
Canavoso, L.E., Frede, S., Rubiolo, E.R., 2004a. Metabolic pathways for dietary lipids in the midgut of hematophagous *Panstrongylus megistus* (Hemiptera: Reduviidae). Insect Biochem. Mol. Biol. 34, 845–854.
Canavoso, L.E., Yun, H.K., Jouni, Z.E., Wells, M.A., 2004b. Lipid transfer particle mediates the delivery of diacylglycerol from lipophorin to fat body in larval Manduca sexta. J. Lipid Res. 45, 456–465.
Chi, S.L., Pizzo, S.V., 2006. Cell surface F_1F_o ATP synthase: a new paradigm? Ann. Med. 38, 429–438.
Chino, H., Downer, R.G., Takahashi, K., 1977. The role of diacylglycerol-carrying lipoprotein I in lipid transport during insect vitellogenesis. Biochim. Biophys. Acta 487, 508–516.
Dantuma, N.P., Van Marrewijk, W.J.A., Wynne, H.J., Van der Horst, D.J., 1996. Interaction of an insect lipoprotein with its binding site at the fat body. J. Lipid Res. 37, 1345–1355.
Dantuma, N.P., Pijnenburg, M.A., Diederen, J.H.B., Van der Horst, D.J., 1997. Developmental down-regulation of receptor-mediated endocytosis of an insect lipoprotein. J. Lipid. Res. 38, 254–265.
Dantuma, N.P., Potters, M., De Winther, M.P.J., Tensen, C.P., Kooiman, F.P., Bogerd, J., Van der Horst, D.J., 1999. An insect homolog of the vertebrate very low density lipoprotein receptor mediates endocytosis of lipophorins. J. Lipid Res. 40, 973–978.
Downer, R.G.H., Chino, H., 1985. Turnover of protein and diacylglycerol components of lipophorin in insect hemolymph. Insect Biochem 15, 627–630.
Eugster, C., Panáková, D., Mahmoud, A., Eaton, S., 2007. Lipoprotein-heparan sulfate interactions in the Hh pathway. Dev. Cell. 13, 57–71.
Folch, J., Lees, M., Sloane Stanley, G.H., 1957. A simple method for isolation and purification of total lipids from animal tissues. J. Biol. Chem. 226, 497–509.
Fruttero, L.L., Rubiolo, E.R., Canavoso, L.E., 2009. Biochemical and cellular characterization of lipophorin-midgut interaction in the hematophagous *Panstrongylus megistus* (Hemiptera: Reduviidae). Insect Biochem. Mol. Biol. 39, 322–331.
Fruttero, L.L., Frede, S., Rubiolo, E.R., Canavoso, L.E., 2011. The storage of nutritional resources during vitellogenesis of *Panstrongylus megistus* (Hemiptera: Reduviidae): the pathways of lipophorin in lipid delivery to developing oocytes. J. Insect Physiol. 57, 475–486.
Galetto, L., Bosco, D., Balestrini, R., Genre, A., Fletcher, J., Marzachì, C., 2011. The major antigenic membrane protein of "Candidatus Phytoplasma asteris" selectively interacts with ATP synthase and actin of leafhopper vectors. PLoS One 6, e22571.
Giot, L., Bader, J.S., Brouwer, C., Chaudhuri, A., Kuang, B., Li, Y., Hao, Y.L., Ooi, C.E., Godwin, B., Vitols, E., et al., 2003. A protein interaction map of *Drosophila melanogaster*. Science 302, 1727–1736.
Grillo, L.A.M., Pontes, E.G., Gondim, K.C., 2003. Lipophorin interaction with the midgut of *Rhodnius prolixus*: characterization and changes in binding capacity. Insect Biochem. Mol. Biol. 33, 429–438.
Hermanson, G., 1996. Antibody modification and conjugation. In: Bioconjugate Techniques. Academic Press, San Diego, pp. 456–493.
Jacquet, S., Malaval, C., Martinez, L.O., Sak, K., Rolland, C., Perez, C., Nauze, M., Champagne, E., Tercé, F., Gachet, C., Perret, B., Collet, X., Boeynaems, J.M., Barbaras, R., 2005. The nucleotide receptor P2Y13 is a key regulator of hepatic high-density lipoprotein (HDL) endocytosis. Cell Mol. Life Sci. 62, 2508–2515.
Krishnamoorthy, M., Jurat-Fuentes, J.L., McNall, R.J., Andacht, T., Adang, M.J., 2007. Identification of novel Cry1Ac binding proteins in midgut membranes from *Heliothis virescens* using proteomic analyses. Insect Biochem. Mol. Biol. 37, 189–201.
Laemmli, U.K., 1970. Cleavage of structural proteins during the assembly of the head of bacteriophage T4. Nature 227, 680–685.
Lee, C.S., Han, J.H., Lee, S.M., Hwang, J.S., Kang, S.W., Lee, B.H., Kim, H.R., 2003. Wax moth, *Galleria mellonella* fat body receptor for high-density lipophorin (HDLp). Arch. Insect Biochem. Physiol. 54, 14–24.
Lin, X., Kim, Y.A., Lee, B.L., Söderhäll, K., Söderhäll, I., 2009. Identification and properties of a receptor for the invertebrate cytokine astakine, involved in hematopoiesis. Exp. Cell Res. 315, 1171–1180.
Martin-Nizard, F., Richard, B., Torpier, G., Nouvelot, A., Fruchart, J.C., Duthilleul, P., Delbart, C., 1987. Analysis of phospholipid transfer during HDL binding to platelets using a fluorescent analog of phosphatidylcholine. Thromb. Res. 46, 811–825.

Martinelli, A.H.S., Kappaun, K., Ligabue-Braun, R., Defferrari, M.S., Piovesan, A.R., Staniscuaski, F., Demartini, D.R., Verli, H., Dal Belo, C.A., Almeida, C.G., Follmer, C., Carlini, C.R., Pasquali, G., 2014. Structure-function studies on Jaburetox, a recombinant insecticidal and antifungal peptide derived from jack bean (*Canavalia ensiformis*) urease. Biochim. Biophys. Acta 1840, 935–944.

Martinez, L.O., Jacquet, S., Esteve, J.P., Rolland, C., Cabezón, E., Champagne, E., Pineau, T., Georgeaud, V., Walker, J.E., Tercé, F., Collet, X., Perret, B., Barbaras, R., 2003. Ectopic beta-chain of ATP synthase is an apolipoprotein A-I receptor in hepatic HDL endocytosis. Nature 421, 75–79.

Martinez, L.O., Jacquet, S., Tercé, F., Collet, X., Perret, B., Barbaras, R., 2004. New insight on the molecular mechanisms of high-density lipoprotein cellular interactions. Cell. Mol. Life Sci. 61, 2343–2360.

Meier, T., Faraldo-Gomez, J., Börsch, B., 2011. ATP synthase-a paradigmatic molecular machine. In: Frank, J. (Ed.), Molecular Machines in Biology. Cambridge Univ. Press, Cambridge, pp. 208–238.

Núñez, J.A., Segura, E.L., 1987. Rearing of Triatominae. In: Brenner, R.R., Stoka, A.M. (Eds.), Chagas' Disease Vectors, vol. II. CRC Press, Boca Raton, pp. 31–40.

Parra-Peralbo, E., Culi, J., 2011. *Drosophila* lipophorin receptors mediate the uptake of neutral lipids in oocytes and imaginal disc cells by an endocytosis-independent mechanism. PLoS Genet. 7, e1001297.

Röhrl, C., Stangl, H., 2013. HDL endocytosis and resecretion. Biochim. Biophys. Acta 1831, 1626–1633.

Sakudoh, T., Iizuka, T., Narukawa, J., Sezutsu, H., Kobayashi, I., Kuwazaki, S., Banno, Y., Kitamura, A., Sugiyama, H., Takada, N., Fujimoto, H., Kadono-Okuda, K., Mita, K., Tamura, T., Yamamoto, K., Tsuchida, K., 2010. A CD36-related transmembrane protein is coordinated with an intracellular lipid-binding protein in selective carotenoid transport for cocoon coloration. J. Biol. Chem. 285, 7739–7751.

Sakudoh, T., Kuwazaki, S., Iizuka, T., Narukawa, J., Yamamoto, K., Uchino, K., Sezutsu, H., Banno, Y., Tsuchida, K., 2013. CD36 homolog divergence is responsible for the selectivity of carotenoid species migration to the silk gland of the silkworm *Bombyx mori*. J. Lipid Res. 54, 482–495.

Schofield, C.J., Jannin, J., Salvatella, R., 2006. The future of Chagas' disease control. Trends Parasitol. 22, 583–588.

Tsuchida, K., Wells, M.A., 1990. Isolation and characterization of a lipoprotein receptor from the fat body of an insect, *Manduca sexta*. J. Biol. Chem. 265, 5761–5767.

Tufail, M., Takeda, M., 2009. Insect vitellogenin/lipophorin receptors: molecular structures, role in oogenesis, and regulatory mechanisms. J. Insect Physiol. 55, 87–103.

Van Antwerpen, R., Linnemans, W.A., Van der Horst, D.J., Beenakkers, A.M.Th, 1988. Immunocytochemical localization of lipophorins in the flight muscles of the migratory locust (*Locusta migratoria*) at rest and during flight. Cell Tissue Res. 252, 661–668.

Van der Horst, D.J., Roosendaal, S.D., Rodenburg, K.W., 2009. Circulatory lipid transport: lipoprotein assembly and function from an evolutionary perspective. Mol. Cell. Biochem 326, 105–119.

Van Hoof, D., Rodenburg, K.W., Van der Horst, D.J., 2005. Receptor-mediated endocytosis and intracellular trafficking of lipoproteins and transferrin in insect cells. Insect Biochem. Mol. Biol. 35, 117–128.

Vantourout, P., Radojkovic, C., Lichtenstein, L., Pons, V., Champagne, E., Martinez, L.O., 2010. Ecto-F_1-ATPase: a moonlighting protein complex and an unexpected apoA-I receptor. World. J. Gastroenterol. 16, 5925–5935.

Via, D.P., Smith, L.C., 1986. Fluorescent labeling of lipoproteins. Methods Enzymol. 129, 848–857.

Walker, J.E., 1998. ATP synthesis by rotary catalysis. Angew. Chem. Int. Ed. 37, 2309–2319.

Zalewska, M., Kochman, A., Estève, J.P., Lopez, F., Chaoui, K., Susini, C., Ozyhar, A., Kochman, M., 2009. Juvenile hormone binding protein traffic – interaction with ATP synthase and lipid transfer proteins. Biochim. Biophys. Acta 1788, 1695–1705.

Ziegler, R., Van Antwerpen, R., 2006. Lipid uptake by insect oocytes. Insect Biochem. Mol. Biol. 36, 264–272.